Mechanics & Industry **21**, 111 (2020)
© AFM, EDP Sciences 2020
https://doi.org/10.1051/meca/2019084

Mechanics & Industry

Available online at:
www.mechanics-industry.org

Regular Article

# Temperature rise characteristics of the valve-controlled adjustable damping shock absorber

Fangwei Xie[1,2,*], Jinxin Cao[2], Erming Ding[2], Kuaidi Wan[2], Xinshi Yu[2], Jun Ke[2], and Kuidong Gao[3]

[1] School of Mechatronic Engineering, China University of Mining and Technology, Xuzhou, PR China
[2] School of Mechanical Engineering, Jiangsu University, Zhenjiang, PR China
[3] Shandong Province Key Laboratory of Mine Mechanical Engineering, Shandong University of Science and Technology, Qingdao, PR China

Received: 20 December 2018 / Accepted: 26 November 2019

**Abstract.** The thermodynamic study of the valve-controlled adjustable damping shock absorber is conducted in order to solve the problem of oil leakage caused by excessive temperature rise of shock absorber. In this paper, the temperature rise of the valve-controlled adjustable damping shock absorber is analyzed from the perspective of energy conservation. Combined with the theory of fluid mechanics, the damping heat model is established, and the heat dissipation model of the shock absorber is established based on heat convection, heat conduction and heat radiation. The corresponding thermal equilibrium equation is established on the basis of damping heat and heat dissipation. The effects of vibration velocity, outer diameter, thickness and length of reservoir cylinder, and wind velocity on its thermal performance have been investigated. Specifically, temperature after thermal equilibrium will grow with the increase of vibration velocity and thickness of reservoir cylinder and degrade with the increase of outer diameter, length of reservoir cylinder and wind velocity. The higher the balance temperature, the shorter time is required to arrive thermal equilibrium. The difference between the experimental and simulation values of oil temperature after thermal equilibrium was not more than 2 °C, which verified the correctness of the theoretical model, while the experimental value in the process of temperature rise lagged behind the simulation value, which was mainly caused by the cumulative error of step-by-step iteration and the mechanical hysteresis in the experiment. The conclusions obtained can provide some references for the design of shock absorbers.

**Keywords:** Adjustable damping / shock absorber / temperature rise / thermal equilibrium

## 1 Introduction

The valve-controlled adjustable damping shock absorber can change damping according to road conditions so that the vehicle has the best driving stability and comfort. It is a significant research direction of the vehicle suspension control system. The thermodynamic study related to the valve-controlled adjustable damping shock absorber is of great significance for improving its stability and reliability in practical applications. Oil leakage and abnormal noise are the most common failure forms of hydraulic shock absorbers according to the after-sales services and maintenance statistics [1,2]. After disassembling the problematic damper and testing its damping force, it is found that the damping force is much smaller than the specified value in the manufacturer's instructions and presents the distortion phenomenon of 'displacement without damping'. The reason is that the viscosity of the oil is extremely sensitive to temperature, the viscosity will decrease dramatically, resulting in the leakage of oil under pressure, and ultimately causing vibration impulse events which trigger abnormal noise. At present, the problem of oil leaking caused by excessive temperature rise has become a key issue in boosting the reliability of the damper. Therefore, it is of great practical value to conduct in-depth research on the characteristics of temperature rise of the shock absorber to improve its quality and reduce the incidence of oil leakage.

Scholars from various countries have studied the energy dissipation and temperature of the shock absorber, mainly in the aspects of thermodynamics and thermo-mechanical coupling dynamics modeling, and put forward the related theoretical concepts, key performance indicators and carried on the related experiments to the relative index [3]. He et al. [4] modeled the damping force of the double-tube shock absorber and analyzed the relationship between damping and temperature change. Yang [5] analyzed the

* e-mail: xiefangwei@163.com

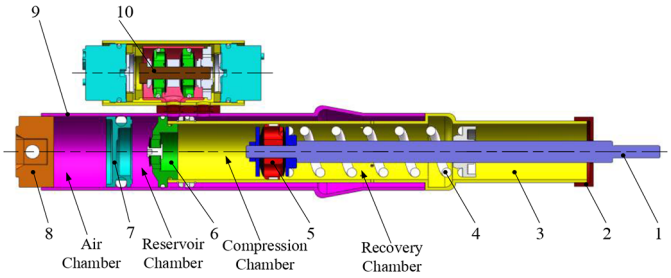


**Fig. 1.** Sketch of valve-controlled damping adjustable shock absorber. 1 – piston rod; 2 – seal assembly; 3 – piston cylinder; 4 – spring assembly; 5 – piston valve assembly; 6 – bottom valve assembly; 7 – floating piston; 8 – plug; 9 – reservoir cylinder; 10 – damping regulating valve.

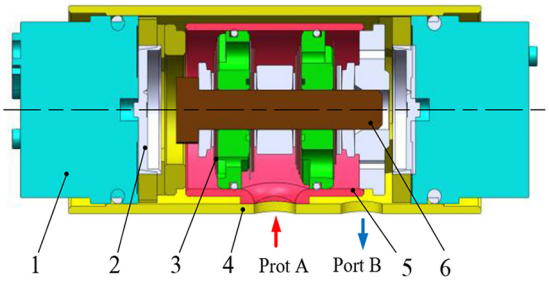


**Fig. 2.** Structural diagram of damping regulating valve assembly. 1 – electromagnet; 2 – two electromagnetic plate valve; 3 – one-way throttle group; 4 – external cylinder; 5 – internal cylinder; 6 – bolt.

thermal and dynamic coupling relationship of a double-tube shock absorber and obtained the surface temperature rise process of the shock absorber under sinusoidal and random excitation. Zhang et al. [6] calculated and simulated the influence of temperature on the damping and vibration characteristics of automobile suspension. Sorniotti [7] established a model for the relationships between the temperature change of the orifice and the pressure difference and flow velocity. Singh and Bera [8] established the thermal model of the double-tube shock absorber and collected the temperature of the outer surface of the main cylinder, which verified the existence of heat transfer to the surrounding environment. Singh and Bera [9] developed a thermal model for the twin-tube hydraulic shock absorber using bond graph approach. Demić and Diligenski [10] attempted to analyze a conversion of mechanical work into heat energy by use of a method of dynamic simulation. Nikolay [11] analyzed the damping changes caused by the surrounding environment of the shock absorber and its own temperature change, and gave the law of the damping characteristics changing with the external temperature. Zhang et al. [12] developed finite element analysis and the experiments for the simulation models with parameters identified of a novel regenerative shock absorber. Qiu et al. [13] established the mathematical model of shock absorber based on the actual structure of anti-snake shock absorber and the related theories of hydraulic fluid mechanics. Xin et al. [14] proposed a shear-valve mode MRF damper for pipeline vibration control and established the dynamic model and the state equation of the pipeline.

Liu et al. [15] established a damping characteristic model for a single-tube inflatable damper and concluded that the increase in density and viscosity of the oil increases the damping of the shock absorber in varying degrees.

In this paper, the mathematical model of the damping of the shock absorber is established, and the heat dissipation process is analyzed based on the heat transfer theory. The thermal equilibrium equation is established by synthesizing the factors of damping heating and heat transfer, and the influence of relevant structural parameters on the thermodynamic characteristics of the shock absorber is analyzed. Simultaneously, the shock absorber is loaded with different loads, the oil temperature is measured and recorded, and the temperature rise curve of the shock absorber is plotted with the shock absorber test bench, and the mathematical model of thermal equilibrium is validated by comparing with the theoretical results.

## 2 Structure and operational principle

This paper studies a valve-controlled adjustable damping shock absorber with an external regulating valve, which is developed on the basis of the double-cylinder hydraulic shock absorber. Figure 1 shows the structure of the shock absorber. The shock absorber can be divided into two parts: the main shock absorber and the damping regulating valve. Damping regulating valve is the key component of damping adjustment, providing four values of damping. The section structure of the damper regulating valve is shown in Figure 2. There are two electromagnets and two electromagnetic plate valves at both ends to control the on and off of the oil circuits. Four sets of one-way throttle groups are installed in the internal cylinder to achieve the flow of oil between the port A and the port B. When the movement of the piston rod forces fluid to flow through the orifice, the gap orifice or the valve port into the other chamber, a throttling effect is created, thereby forming a damping force.

According to the structure and composition of the valve-controlled adjustable damping shock absorber described above, the operational principle of the damper can be described by the schematic diagram shown in Figure 3. The displacement of the piston rod relative to the piston cylinder under the external excitation causes the volume of one chamber to become smaller while the volume of the other chamber increases. The oil in the reduced volume chamber is squeezed and flows through the corresponding orifice to the increased volume chamber under the squeezing. Usually, according to the relative motion relationship between the piston rod and main cylinder, the working process is divided into compression stroke and recovery stroke. The damping forming process of the shock absorber is explained below.

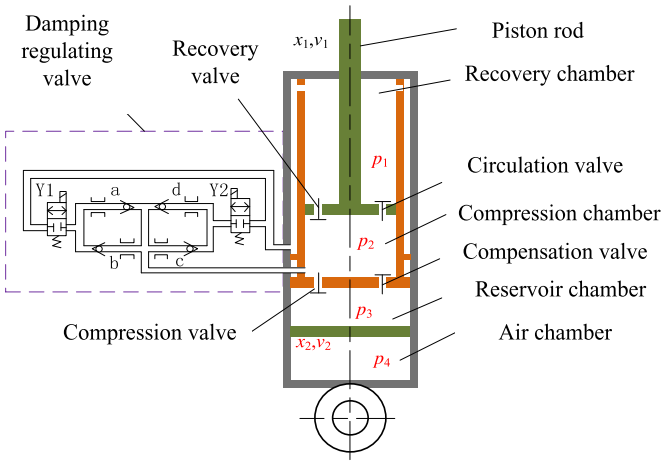


**Fig. 3.** Working principle of valve-controlled damping adjustable shock absorber.

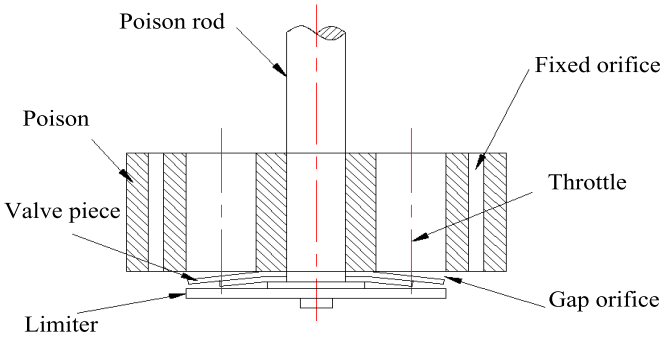


**Fig. 4.** Structure model of piston valve assembly.

Compression stroke: When the piston rod moves downward under the external excitation, the piston is compressed. The oil in the compression chamber is divided into three parts and is squeezed out: a part flows into the recovery chamber through the circulation valve, a part flows into the reservoir cylinder through the compression valve, and a part of the oil flows into the damping regulating valve.

Rebound stroke: when the piston rod moves outward under the action of external excitation, the damper is in the rebound stroke. The oil in the reservoir cylinder flows into the compression chamber, and part of the oil in the recovery chamber flows into the valve port B through the small hole in the piston barrel and the annular gap between the piston cylinder and the reservoir cylinder and then passes through the damping regulating valve.

Figure 4 shows the structure model of piston valve assembly. When the damper is in operation, its working state can be divided into two stages: before opening the valve and after opening the valve. When the vibration velocity of the damper is less than $v_{k1}$, the valve piece is not deformed under the pressure of oil, that is, the pre-opening stage; when the vibration velocity exceeds $v_{k1}$, the valve piece is deformed under the pressure of oil, that is, the post-opening stage.

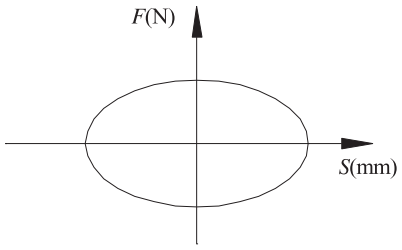


**Fig. 5.** Indicator diagram of the shock absorber.

During the operation of the damper, the heat balance of the damper is mainly affected by two aspects, namely the heating power and the heat dissipation power of the damper. The cause of the damper's heating is its damping force, which directly results in an increase in temperature. The heat dissipation process of the damper is a heat exchange process between the internal energy of the damper and the energy of the external environment, which is manifested by a decrease in the overall temperature of the damper.

## 3 Temperature rise and simulation analysis of valve-controlled adjustable damping shock absorber

### 3.1 Heating model of damping

Usually, the damping force can be measured by the test bench and the performance of the shock absorber can be described by the indicator diagram as shown in Figure 5.

Damping characteristic of damper indicator diagram is the comprehensive performance of throttling characteristic of the damper valve system. Since its abscissa is displacement and the ordinate corresponds to damping force, the area enclosed by the indicator diagram can be used as the work done by damping force, i.e. heating capacity in each cycle.

In the actual working process, the damping force of the damper is mainly composed of the throttle pressure difference of the damping oil passing through the orifice and the friction between the piston and the cylinder. At the same time, changes in parameters such as external temperature, friction inside the cylinder, and flow state of the oil also affect the damping characteristics all the time. If all factors are considered during modeling, it will make the model too complicated to solve. Therefore, in order to simplify the model, some corresponding assumptions were made during the mathematical modeling [16]. The specific conditions are as follows:

- Assuming that the shock absorber is well sealed and there is no leakage.
- Assuming that the floating piston is well sealed and the phenomenon of gas dissolving into the oil is not considered.
- Ignoring the elastic deformation of the cylinder, piston rod, piston and other parts.
- Assuming that the pressures in the same chamber are equal during the working process.

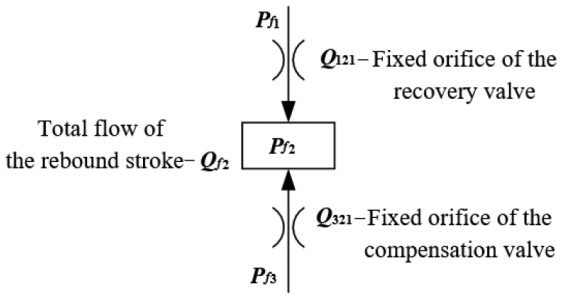


**Fig. 6.** Oil flow model of recovery stroke before valve opening.

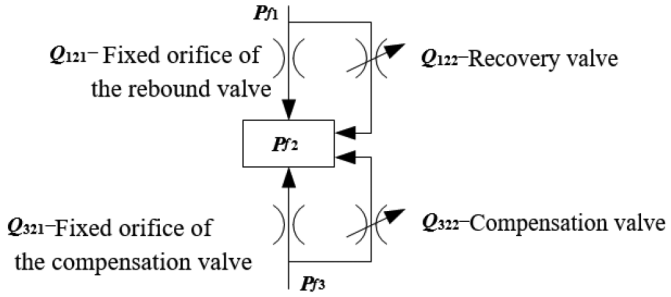


**Fig. 7.** Oil flow model of recovery stroke after valve opening.

### 3.1.1 Rebound stroke

#### *3.1.1.1 Before opening the valve*

When the vibration velocity received by the damper is not high, the recovery valve is in the pre-opening state, and the damping force at this time is generated by the fixed orifice. The oil flow schematic is shown in Figure 6.

We define

$$a_1 = C_v A_{fg}\sqrt{2/\rho}, \quad a_2 = C_v A_{bg}\sqrt{2/\rho}. \tag{1}$$

Substituting the corresponding formulas, we get $F_{fkq}$ [17]:

$$F_{fkq} = \left[\frac{\pi\left(d_p^2 - d_r^2\right)}{4a_1} v_{f1}\right]^2 \times A_p - \left\{\frac{P_{40}V_{40}}{V_{40} + A_c x_{f2}} - \left(\frac{\pi d_r^2}{4a_2} v_{f1}\right)^2 + \left[\frac{\pi\left(d_p^2 - d_r^2\right)}{4a_1} v_{f1}\right]^2\right\} A_r. \tag{2}$$

#### *3.1.1.2 After opening the valve*

The flow of the circuit after opening the valve is shown in Figure 7. In the following, only the throttling characteristics formed by the deformation gap of the superimposed valve sheets are modeled.

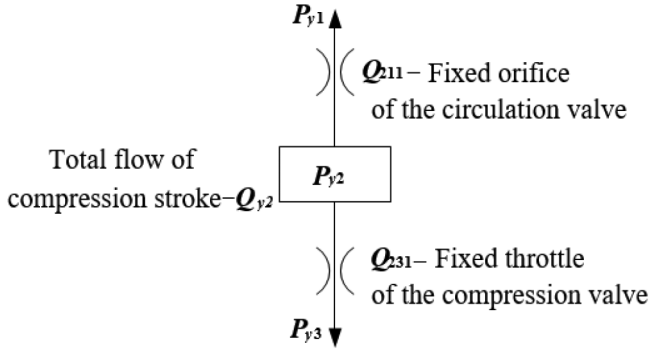


**Fig. 8.** Oil flow model of compression stroke before valve opening.

We define

$$a_3 = \frac{\pi\delta_f^3}{6\mu\ln\left(r_{f2}/r_{f1}\right)}, \quad a_4 = \frac{\pi\delta_b^3}{6\mu\ln(r_{b2}/r_{b1})}. \tag{3}$$

Find out the damping force after the opening valve $F_{fkh}$ [11] is:

$$F_{fkh} = \frac{P_{40}V_{40}}{V_{40} + A_c x_{f2}} - \frac{Q_{f3}}{a_4} - \frac{a_2\left(a_2 - \sqrt{a_2^2 + 4a_4 Q_{f3}}\right)}{2a_4^2} + \frac{Q_{f1}}{a_3} + \frac{a_1\left(a_1 - \sqrt{a_1^2 + 4a_3 Q_{f1}}\right)}{2a_3^2}. \tag{4}$$

### 3.1.2 Compression stroke

#### *3.1.2.1 Before opening the valve*

The shock absorber is in the pre-opening state of the compression stroke, and the corresponding oil flow as shown in Figure 8.

We define

$$b_1 = C_v A_{lg}\sqrt{2/\rho}, \quad b_2 = C_v A_{yg}\sqrt{2/\rho}. \tag{5}$$

Similarly, the damping force $F_{ykq}$ before opening the valve can be analyzed [11]:

$$F_{ykq} = \left[\frac{\pi\left(d_p^2 - d_r^2\right)}{4b_1} v_{y1}\right]^2 \times A_p + \left\{\frac{P_{40}V_{40}}{V_{40} - A_c x_{y2}} + \left(\frac{\pi d_r^2}{4b_2} v_{y1}\right)^2 - \left[\frac{\pi\left(d_p^2 - d_r^2\right)}{4b_1} v_{y1}\right]^2\right\} A_r. \tag{6}$$

#### *3.1.2.2 After opening the valve*

The corresponding oil flow after opening the valve is shown in Figure 9. In the following, only the throttling

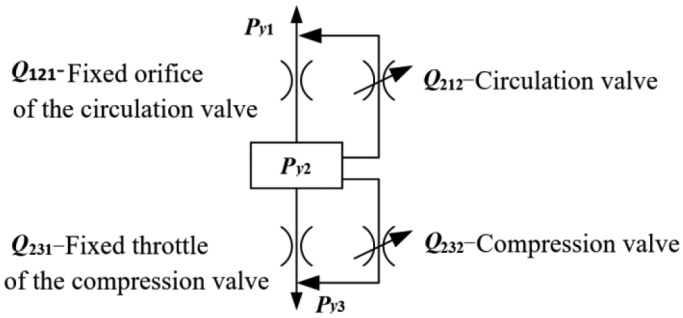


**Fig. 9.** Oil flow model of compression stroke after valve opening.

characteristics formed by the deformation gap of the superimposed valve sheets are modeled.

We define

$$b_3 = \frac{\pi\delta_l^3}{6\mu\ln(r_{l2}/r_{l1})}, \quad b_4 = \frac{\pi\delta_y^3}{6\mu\ln(r_{y2}/r_{y1})}. \tag{7}$$

Therefore, the damping force after opening the valve of the compression stroke is $F_{ykh}$ [11]:

$$F_{ykh} = \left[\frac{Q_{y1}}{b_3} + \frac{b_1\left(b_1 - \sqrt{b_1^2 + 4b_3Q_{y1}}\right)}{2b_3^2}\right]^2 \times A_p + \left[\frac{P_{40}V_{40}}{V_{40} - A_c x_{y2}} + \frac{Q_{y3}}{b_4} + \frac{b_2\left(b_2 - \sqrt{b_2^2 + 4b_4Q_{y3}}\right)}{2b_4^2} - \frac{Q_{y1}}{b_3} - \frac{b_1\left(b_1 - \sqrt{b_1^2 + 4b_3Q_{y1}}\right)}{2b_3^2}\right] A_r. \tag{8}$$

### 3.2 Heat dissipation process analysis

Before establishing the overall heat dissipation model, it is assumed that the viscosity of the oil is constant at each working cycle during simulation and the damping force is all converted into the internal energy of the oil.

The heat conduction coefficient of the valve-controlled adjustable damping shock absorber is considered as constant [18], and only the temperature variation in the radial direction of the damper is considered, which leads to one-dimensional steady state heat conduction.

The heat flux of the heat transfer on the wall of the work cylinder is:

$$\Phi_n = \frac{2\pi\lambda_g l_n(T_{n1} - T_{n2})}{\ln(r_{n1}/r_{n2})}. \tag{9}$$

The heat flux of the reservoir cylinder is:

$$\Phi_w = \frac{2\pi\lambda_g l_w(T_{w1} - T_{w2})}{\ln(r_{w2}/r_{w1})}. \tag{10}$$

The heat flux of oil in the reservoir chamber is:

$$\Phi_{cy} = \frac{2\pi\lambda_y l_{cy}(T_{w1} - T_{n2})}{\ln(r_{w2}/r_{w1})}. \tag{11}$$

The thermal resistance of shock absorber is:

$$R_{cd} = \frac{1}{2\pi\lambda_g l_n}\ln\frac{r_{n1}}{r_{n2}} + \frac{1}{2\pi\lambda_g l_w}\ln\frac{r_{w1}}{r_{w2}} + \frac{1}{2\pi\lambda_y l_{cy}}\ln\frac{r_{w1}}{r_{n2}}. \tag{12}$$

The heat transfer process of the oil in the working cylinder is forced-convection heat transfer. The heat transfer model can be expressed as:

$$\Phi_{dl} = h_{dl}A_n(T_y - T_{n1}). \tag{13}$$

The heat transfer coefficient of the outer surface of the reservoir cylinder [19] is:

$$h_{kq} = \frac{\lambda_{kq}}{l_w}\left\{0.825 + \frac{0.387(GrPr_{kq})^{1/6}}{[1 + (0.492/Pr_{kq})^{9/16}]^{8/27}}\right\}^2. \tag{14}$$

The thermal resistance of heat convection is:

$$R_{dl} = \frac{1}{h_{dl}A_n}. \tag{15}$$

The radiant heat flux on the surface of the reservoir cylinder of the shock absorber is:

$$\Phi_r = \varepsilon c_b A_w \frac{T_{w2}^4 - T_{\text{air}}^4}{100^4}. \tag{16}$$

The radiation heat transfer coefficient $h_r$ of the external surface of the damping cylinder is obtained as follows:

$$h_r = \varepsilon c_b \frac{(T_{w2}^2 + T_{\text{air}}^2)(T_{w2} + T_{\text{air}})}{100^4}. \tag{17}$$

The surface heat transfer coefficient of the external surface of shock absorber $h_b$ is:

$$h_b = h_{kq} + h_r. \tag{18}$$

Therefore, the thermal resistance $R_b$ of the heat transfer from the surface of the reservoir cylinder is:

$$R_b = 1/(h_b \bullet A_w). \tag{19}$$

The total heat flow expression in the heat transfer process of the shock absorber can be obtained by the above thermodynamic analysis:

$$Q_z = (T_y - T_{\text{air}})/R_z. \tag{20}$$

## 4 Simulation of temperature rise characteristics

### 4.1 Parameter setting

The excitation of the shock absorber is the sinusoidal signal with the amplitude value $A_m = 37.5$ mm. The

**Table 1.** Geometric parameters of the shock absorber.

| Name | Parameter | Name | Parameter |
|---|---|---|---|
| Diameter of piston cylinder (mm) | 36 | Diameter of recovery valve (mm) | 8 |
| Diameter of the piston rod (mm) | 15 | Number of recovered valve holes | 2 |
| Diameter of reservoir cylinder (mm) | 45 | Diameter of flow valve (mm) | 8 |
| Wall thickness (mm) | 2 | Number of recovery valves | 4 |
| Diameter of compression valve (mm) | 3 | Diameter of compensation valve (mm) | 5 |
| Number of compressed valve holes | 4 | Number of compensation valves | 4 |
| Length of the piston cylinder (mm) | 175 | Length of reservoir cylinder (mm) | 365 |

**Table 2.** Physical parameters of oil and material (25 °C).

| Name | Parameter | Name | Parameter |
|---|---|---|---|
| Viscosity of oil ($m^2/s$) | $3.5 \times 10^{-6}$ | Specific heat of oil ($J/(kg \cdot K)$) | $1.88 \times 10^{-3}$ |
| Density of oil ($kg/m^3$) | 875 | Thermal conductivity of air ($W/(m \cdot K)$) | $2.76 \times 10^{-2}$ |
| Thermal conductivity of oil ($W/(m \cdot K)$) | 0.145 | Thermal conductivity of cylinder wall ($W/(m \cdot K)$) | 51 |

corresponding excitation frequencies are set at 0.556 Hz, 1.112 Hz, 1.668 Hz and 2.207 Hz respectively according to the vibration velocity $V_m$ of 0.052 m/s, 0.13 m/s, 0.262 m/s and 0.524 m/s. The relevant parameters of the shock absorber are shown in Tables 1 and 2.

The viscosity-temperature equation [20] of a certain type of hydraulic oil is selected as follows:

$$\mu = 0.0806e^{-0.059T}. \quad (21)$$

## 4.2 Temperature rise characteristics

During the operation of the shock absorber, the thermal equilibrium of the shock absorber is mainly affected by two aspects, namely the heating power of the shock absorber and the heat dissipation power of the shock absorber. The cause of the shock absorber's heating is its damping force, which directly results in an increase in temperature. The heat dissipation process of the shock absorber is a heat exchange process between the internal energy of the shock absorber and the internal energy of the external environment, which is manifested as a decrease in the overall temperature. In the analysis and calculation, each working cycle of the shock absorber is used as the calculation unit, and the shock absorber first causes the temperature to rise due to the work of the damping force, and then the heat dissipation process is calculated due to the existence of the temperature difference. The final temperature rise is obtained by a iteration calculation of "heat generation − heat dissipation − heat generation". The Matlab simulation program is written to obtain the shock absorber heat balance curve according to the equations and parameters established in 3.1, 3.2 and 4.1.

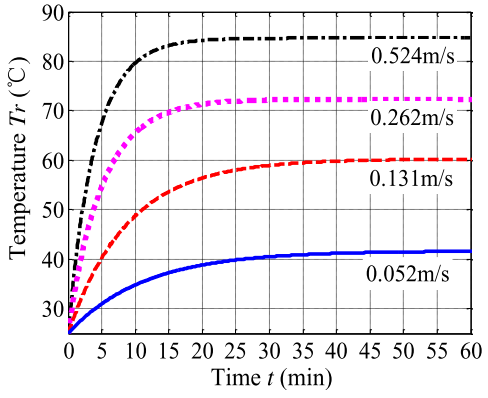


**Fig. 10.** Thermal equilibrium characteristics at different velocities.

### 4.2.1 Impact of vibration velocity *v* on thermal equilibrium

The temperature rise curves at four vibration velocity can be obtained by changing the vibration velocity and simulating the thermal equilibrium of the damper. The results are shown in Figure 10.

Comparing each simulation curve of Figure 10, we can find that the oil temperature $T_r$ rises rapidly in a certain period in the beginning, but the temperature changes slowly and eventually does not change with the passage of time, that is, it can always reach a certain balanced temperature. This illustrates the correctness of the analysis of the damping heating process and the heat dissipation process. The temperature of the vibration from small to large corresponds to the balance temperature of 42.67 °C, 60.59 °C, 72.37 °C and 84.25 °C, the corresponding time to

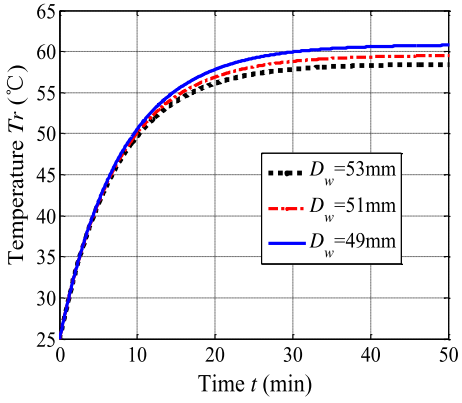


**Fig. 11.** Thermal equilibrium characteristics with varied $D_w$.

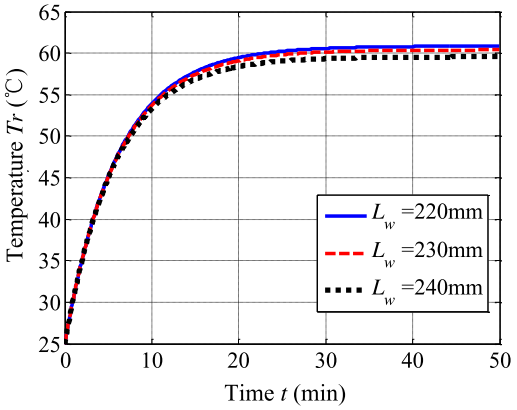


**Fig. 13.** Thermal equilibrium characteristics with varied $l_w$.

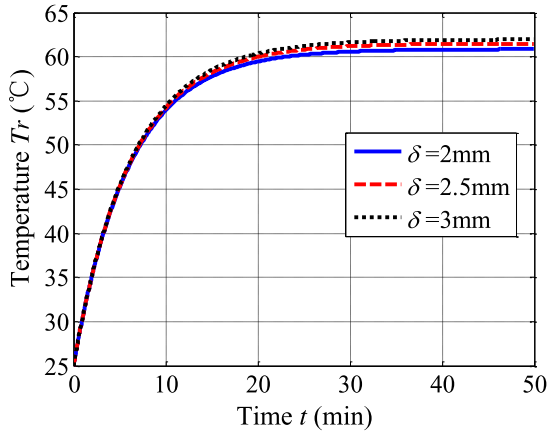


**Fig. 12.** Thermal equilibrium characteristics with varied $\delta$.

thermal equilibrium is about 55 min, 45 min, 35 min and 25 min, respectively. That is to say, the balance temperature is gradually increasing, but the time required is decreasing with the increase of vibration velocity. It is indicated that a long time running on poor pavement will make the shock absorber reach the thermal equilibrium faster, which will increase the possibility of failure due to the high temperature.

#### 4.2.2 Impact of the outer diameter $D_w$ of the reservoir cylinder on the thermal equilibrium

To improve the heat dissipation performance of the shock absorber, the outer diameter $D_w$ of the absorber is 49 mm, 51 mm and 53 mm with other parameters unchanged, the thermal equilibrium characteristics is simulated under the vibration of $V_m = 0.131$ m/s. The result is shown in Figure 11.

The results from Figure 11 show that with the increase of the outer diameter $D_w$, the temperature of the thermal equilibrium is reduced correspondingly, and the time required for the thermal equilibrium is correspondingly prolonged. This is because the increase of the outer diameter increases the contact area between the the reservoir cylinder and air, thus improving the overall heat dissipation effect of the shock absorber.

#### 4.2.3 Impact of the thickness of the reservoir cylinder on the thermal equilibrium

The shock absorber is simulated under the vibration $V_m = 0.131$ m/s with taking the thickness of reservoir cylinder to 2 mm, 2.5 mm, 3 mm when the other parameters are the same, and the results of its thermal equilibrium process are shown in Figure 12. The results show that increasing the thickness will increase the balance temperature, because increasing the thickness will correspondingly increase the overall thermal resistance of the damper, thereby reducing the effect of the shock absorber radiating outward.

#### 4.2.4 Impact of the length of the reservoir cylinder on the thermal equilibrium

Setting other parameters unchanged, taking the length $l_w$ of reservoir cylinder to 220 mm, 230 mm, 240 mm, simulate the shock absorber under the vibration of $V_m = 0.131$ m/s, get the thermal equilibrium curve of the shock absorber, the result is as shown in Figure 13.

As the result of Figure 13 shows, increasing the length of the reservoir cylinder will reduce the balance temperature, but the temperature difference is not obvious. This is because the increase in the length of the reservoir cylinder will increase the heat dissipation area of the surface, but also increase indirectly the volume of fluid, resulting in the increase of thermal resistance.

#### 4.2.5 Impact of wind velocity on the thermal equilibrium

Setting other parameters unchanged, taking wind velocity $V_w$ as 60 km/h, 100 km/h, 120 km/h, simulation of the shock absorber under the vibration of $V_m = 0.131$ m/s, the result is shown in Figure 14. It can be seen that increasing the wind velocity will increase the airflow around the shock absorber, which improves the heat dissipation condition of the external surface of the shock absorber and then reduces the temperature after the thermal equilibrium.

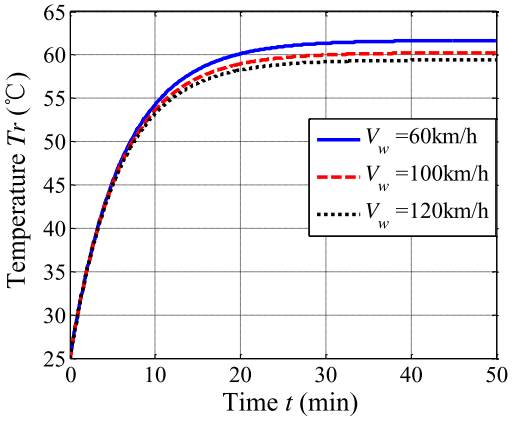


**Fig. 14.** Thermal equilibrium characteristics at $V_w$.

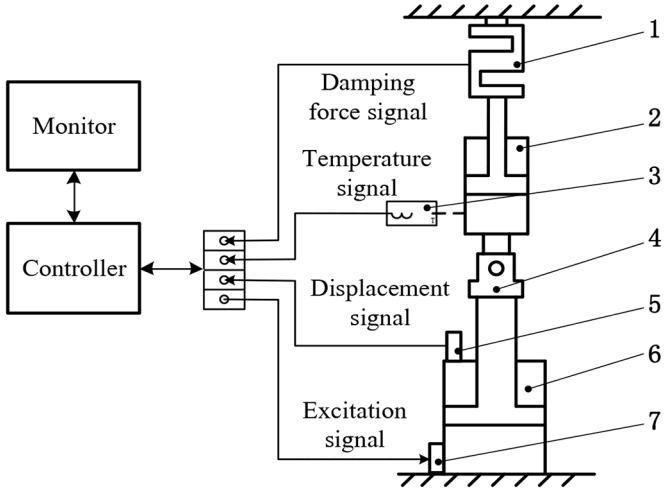


**Fig. 15.** Structural diagram of test bench. 1 – force sensor; 2 – shock absorber; 3 – temperature sensor; 4 – connector; 5 – displacement sensor; 6 – actuator; 7 – servo valve.

## 5 Discussion on the comparison between experimental results and simulation results

The real-time temperature of the oil and the displacement of the piston was measured by the electro-hydraulic servo test bench [21]. The design and construction of the test bench are carried out according to the experimental functional requirements. The structural is shown in Figure 15. The servo test bench is divided into three units of mechanical, hydraulic and electrical control units, wherein the lower base is fixed with an actuator and a displacement sensor. The driving rod of the actuator is connected with the outer cylinder of the shock absorber; the force sensor is connected with the piston rod of the shock absorber, and the pulling rod of the displacement sensor is connected with the outer cylinder of the shock absorber. In addition, a hydraulic valve block is installed to replace damping control valve to drain the oil in the shock absorber and install a temperature sensor. The hydraulic unit is mainly composed of hydraulic power source, a servo valve, an actuator and other pipe fittings. The electrical control unit mainly includes components such as a monitor, a signal acquisition and a processing module.

First, the shock absorber sample is placed in a normal temperature environment for more than 6 hours; then the amplitude and the excitation frequency of the actuator are set to be the same as that of Section 4.1. The specific process of the experiment is as follows:

- Fix the lower end of the shock absorber sample on the servo cylinder of the test bench, so that the upper end of the piston rod is suspended.
- Start the hydraulic power source to provide power to the test bench.
- Input the control drive command in the upper computer, find the middle position by measuring the highest position and the lowest position of the piston rod, and initialize the position of the shock absorber piston rod.
- Connect the upper end of the shock absorber piston rod and the force sensor.
- Input the corresponding sinusoidal excitation signal on the host computer, and set the experimental value every 2 minutes.
- The shock absorber damping force and temperature rise curve can be output after deriving the test results and performing post-processing.

The temperature data corresponding to the vibration velocity is plotted and compared with the simulated values. The results are shown in Figure 16.

According to the simulation and experimental data of Figure 16, it is shown that the temperature of the shock absorber tends to flatten and remain basically unchanged after a period, and the temperature difference after thermal equilibrium does not exceed 2 °C.

From the point of view of temperature rise, the experimental value of the balance temperature is generally smaller than that of the simulation, which is due to the simultaneous occurrence of all directions when the shock absorber is dissipating heat, while only the radial heat dissipation is considered in the simulation. From the point of view of time, the experimental curve lags the simulation curve, which is mainly caused by two aspects: on the one hand, the temperature rise in simulation is based on the step accumulation of 'work- dissipation', but in fact, the damping work and the heat dissipation are carried out simultaneously; On the other hand, the heat transfer and signal acquisition in the experiment need certain response time. In addition, the experimental value of the balance temperature under the velocity of 0.052 m/s was slightly higher than that of the simulation, which was mainly caused by mechanical friction at low speed.

## 6 Conclusions

The thermodynamic balance model of this shock absorber was established on the basis of damping heating and heat dissipation. The effects of vibration velocity, outer diameter, thickness, length of reservoir cylinder, and wind

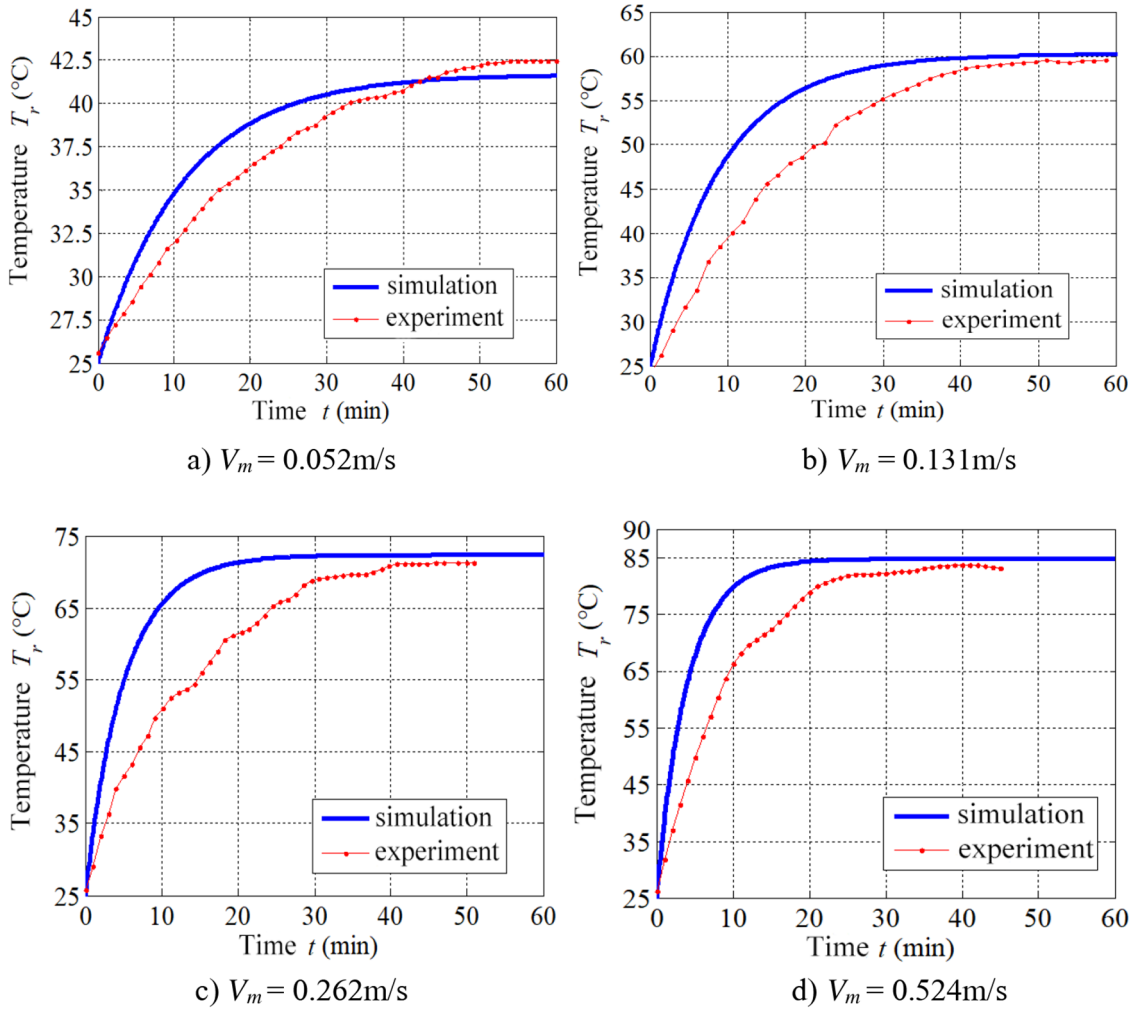


**Fig. 16.** Thermal equilibrium comparison between test and simulation at varied velocities.

velocity on its thermal performance have been investigated. The conclusions obtained can provide some references for the design of shock absorbers. The main conclusions are as follows:

- Temperature after thermal equilibrium will grow with the increase of vibration velocity and reservoir cylinder's thickness and degrade with the increase of outer diameter and length of reservoir cylinder and wind velocity. The higher the balance temperature, the shorter time is required to arrive thermal equilibrium.
- Comparing experiments with simulation, the difference of oil temperature after thermal equilibrium at the same vibration velocity was less than 2 °C and the experimental values lagged simulation which was mainly caused by the accumulated error of stepped iteration in simulation and mechanical hysteresis in experiments. The thermodynamic study related to the valve-controlled adjustable damping shock absorber is of great significance to improve its stability and reliability in practical application.

## Nomenclature

| | |
|---|---|
| $A_{bg}$ | Area of the fixed throttle orifice for compensation valve, $m^2$ |
| $A_c$ | Cross-sectional area of the floating piston, $m^2$ |
| $A_{fg}$ | Area of fixed throttle orifice for recovery valve, $m^2$ |
| $A_{lg}$ | Area of fixed throttle orifice for circulation valve, $m^2$ |
| $A_m$ | Amplitude value, mm |
| $A_n$ | Heat exchange area between the inner wall and the oil, $m^2$ |
| $A_p$ | Area of the piston, $m^2$ |
| $A_r$ | Area of the piston rod, $m^2$ |
| $A_w$ | Radiating area of the reservoir cylinder, $m^2$ |
| $A_{yg}$ | Area of fixed throttle orifice for compression valve, $m^2$ |
| $c_b$ | Radiation coefficient of the reservoir cylinder, $W/(m^2 \cdot K^4)$ |
| $C_v$ | Flow coefficient |
| $d_p$ | Diameter of the piston, m |
| $d_r$ | Diameter of the piston rod, m |

$D_w$ Outer diameter of the reservoir cylinder, mm
$F_{fkq}$ Damping force of the recovery stroke before opening the valve, N
$F_{fkh}$ Damping force of the recovery stroke after opening the valve, N
$F_{ykq}$ Damping force of the recovery stroke before opening the valve, N
$F_{ykh}$ Damping force of the compression stroke after opening the valve, N
$Gr$ Grashof number of air
$h_b$ Surface heat transfer coefficient of the external surface of shock absorber
$h_{dl}$ Heat transfer coefficient of forced convection, $W/(m^2 \cdot K)$
$h_{kq}$ Heat transfer coefficient of the outer surface of the reservoir cylinder
$h_r$ Radiation heat transfer coefficient of the external surface of the damping cylinder
$l_{cy}$ Effective lengths of the overlapping chamber, m
$l_n$ Effective lengths of working cylinder, m
$l_w$ Effective lengths of reservoir cylinder, mm
$P_{40}$ Pre-filling pressure of the gas chamber, Pa
$P_{f1}$ Pressure in the recovery chamber, Pa
$P_{f2}$ Pressure in the compression chamber, Pa
$P_{f3}$ Pressure of the compensating chamber during the recovery stroke, Pa
$P_{rkq}$ Prandtl number of air, Pa
$P_{y1}$ Pressures of the compression chamber, Pa
$P_{y2}$ Pressures of the recovery chamber, Pa
$P_{y3}$ Pressures of gas chamber and compensation chamber, Pa
$Q_{121}$ Flow through the fixed throttle of the circulation valve after valve opening, $m^3/s$
$Q_{122}$ Flow through the recovery valve after valve opening, $m^3/s$
$Q_{211}$ Flow of fixed throttle of the circulation valve, $m^3/s$
$Q_{212}$ Flow through the circulation valve, $m^3/s$
$Q_{231}$ Flow of fixed throttle of the compression valve, $m^3/s$
$Q_{232}$ Flow through the compression valve, $m^3/s$
$Q_{321}$ Flow through the fixed throttle of compensation valve after valve opening, $m^3/s$
$Q_{322}$ Flow through the compensation valve after valve opening, $m^3/s$
$Q_{f1}$ Flow through the recovery chamber in the recovery stroke before opening the valve, $m^3/s$
$Q_{f2}$ Total flow of the recovery stroke, $m^3/s$
$Q_{f3}$ Change of the oil flow of the compensation chamber in the recovery stroke, $m^3/s$
$Q_{y1}$ Change of the oil flow of the compensating chamber, $m^3/s$
$Q_{y2}$ Total flow of compression stroke, $m^3/s$
$Q_{y3}$ Change of the oil flow of the compensating chamber, $m^3/s$
$Q_z$ Total heat flow in the heat transfer process of the shock absorber, W
$r_{f1}$ Inner radius of the recovery valve, m
$r_{f2}$ Outer radius of the recovery valve, m
$r_{n1}$ Internal radius of working cylinder, m
$r_{n2}$ External radius of working cylinder, m
$r_{w1}$ Internal radius of reservoir cylinder, m
$r_{w2}$ External radius of and reservoir cylinder, m
$r_{y1}$ Inside radius of the circulation valve, m
$r_{y2}$ Outside radius of the circulation valve, m
$R_b$ Thermal resistance of the heat transfer of the reservoir cylinder, K/W
$R_{cd}$ Thermal resistance in in the process of heat conduction
$R_{dl}$ Thermal resistance in in the process of heat convection
$R_z$ Thermal resistance in heat transfer process
$T_{\text{air}}$ Temperature of the air, K
$T_{n1}$ Temperatures of inner wall of the working cylinder, K
$T_{n2}$ Temperatures of the outer wall of the working cylinder, K
$T_r$ Oil temperature, °C
$T_{w1}$ Temperatures of the inner walls of the reservoir cylinder, K
$T_{w2}$ Temperatures of the surface of the reservoir cylinder, K
$T_y$ Oil temperature in working cylinder, K
$v$ Vibration velocity, m/s
$v_{f1}$ Speed of the piston during the recovery stroke, m/s
$v_{y1}$ Speed of the piston rod when compressing stroke, m/s
$V_{40}$ Initial volume of the gas chamber in the recovery stroke, $m^3$
$x_{f2}$ Displacement of the damper floating piston during the recovery stroke, m
$x_{y2}$ Displacement of the damper floating piston during the compression stroke, m

Greek symbols

$\rho$ Density of oil, $kg/m^3$
$\mu$ Dynamic viscosity of oil, $Pa \cdot s$
$\delta$ Thickness of reservoir cylinder, mm
$\delta_f$ Bending deformation of the recovery valve, m
$\delta_b$ Bending deformation of the compensation valve, m
$\delta_l$ Bending deformation of the circulation valve, m
$\delta_y$ Bending deformation of the compression valve, m
$\varepsilon$ Emission rate of the external radiation of the reservoir cylinder
$\lambda_g$ Heat conduction coefficients of cylinder, $W/(m \cdot K)$
$\lambda_{kq}$ Heat transfer coefficient of air
$\lambda_y$ Heat conduction coefficients of oil, $W/(m \cdot K)$
$\lambda_{kq}$ Heat transfer coefficient of air, $W/(m \cdot K)$
$\Phi_{dl}$ Convective heat flow
$\Phi_r$ Radiant heat flux, W
$\Phi_n$ Heat flux of the heat transfer on the wall of the work cylinder, W
$\Phi_w$ Heat flux of the reservoir cylinder, W
$\Phi_{cy}$ Heat flux of oil in the reservoir chamber, W

The authors would like to acknowledge the support of the National Natural Science Foundation of China (U1810123), and Open Foundation of Shandong Province Key Laboratory of Mine Mechanical Engineering of Shandong University of Science and Technology (2019KLMM103).

## References


[1] L. Sun, Z. Yang, Competing in the automotive aftermarket-shock absorber articles, Auto Driv. Serv. **48**, 109–113 (2012)

[2] Z. Mu, H. Cao, H. Xu, Discussion on oil leakage of motorcycle front shock absorber, Modern Manufactur. Technol. Equip. **243**, 133–134 ( 2017)

[3] M.S.M. Sani, E. Husin, M.M. Noor, Experimental heat transfer study on the shock absorber operation, in *International Conference on Science and Technology, Applications in Industry and Education*, 2008, pp. 759–765

[4] Q. He, G. Zhang, Q. Ling, L. Yu, Influence of temperature variation on the performance of hydraulic shock absorber, Mach. Tool Hydraulics **30**, 108–110 (2002)

[5] P. Yang, Research on the Mechanism of the Vehicle Hydraulic Shock Absorber, Master, Tongji University, 2004

[6] L. Zhang, Z. Yu, P. Yang, D. Yin, Theoretic investigation on thermodynamics of the vehicle hydraulic shock absorber, J. Vib. Shock **25**, 95–98 (2006)

[7] A. Sorniotti, Shock Absorber Thermal Model: Basic Principles and Experimental Validation, SAE Technical Paper 2008-01-0344, from https://doi.org/10.4271/2008-01-0344, 2008

[8] A. Singh, T.K. Bera, Bond Graph aided thermal, modeling of twin-tube shock absorber, Int. J. Model. Simul. **36**, 183–192 (2016)

[9] A. Singh, T.K. Bera, Bond graph aided thermal modelling of twin-tube shock absorber, Int. J. Model. Simul. **36**, 10 (2016)

[10] M.D. Demić, Đ.M. Diligenski, Numerical simulation of shock absorbers heat load for semi-active vehicle suspension system, Therm. Sci. **20**, 1725–1739 (2016)

[11] P. Nikolay, Influence of shock absorber temperature on vehicle ride comfort and road holding, MATEC Web Conf. **133**, 02006 (2017)

[12] R. Zhang, X. Wang, Z. Liu, A novel regenerative shock absorber with a speed doubling mechanism and its Monte Carlo simulation, J. Sound Vib. **417**, 260–276 (2017)

[13] L. Qiu, S. Jingwei, H.U. Xu et al., External characteristics simulation of high-speed rail anti-snake shock absorber, in *2018 Proceedings of the Annual Meeting of China Automotive Engineering Society*

[14] D.K. Xin, S.L. Nie, H. Ji et al., Characteristics, optimal design, and performance analyses of MRF damper, Shock Vibrat. **2018**, 1–17 (2018)

[15] H. Liu, F. Xie, K. Zhang, X. Zhang, J. Zhang, C. Wang et al., Effect of air chamber and oil properties on damping characteristics of single-tube pneumatic shock absorber, Int. J. Struct. Integr. **9**, 27–37 (2018)

[16] C. Du, Research on Damping Properties of Separated and Manually Adjustable Shock Absorbers Oriented to Damping Matching, Master, Jilin University, 2012

[17] R. Xuan, Research on Valve-controlledAdjustable Damping Shock Absorber and its Damping Characteristics, Master, Jiangsu University, 2016

[18] Y.Y. Pechenegov, O.Y. Pechenegova, Concerning stabilization of heat transfer of a gas-suspension flow in a tube, Heat Transfer Res. **34**, 6 (2003)

[19] K. Everaert, Heat transfer from a single tube to the flowing gas-solid suspension in a CFB riser, Heat Transfer Eng. **27**, 66–70 (2006)

[20] X. Du, H. Chen, Y. Li et al., The study on the performance of the great wall SAF AS shock absorber oil, Hydraul. Pneum. Seals **35**, 1–5 (2015)

[21] F. Xie, R. Xuan, B. Zhang et al., Design and experimental study of test bench for damping adjustable shock absorber based on xPC, Autom. Technol. **483**, 44–48 (2015)


**Cite this article as**: F. Xie, J. Cao, E. Ding, K. Wan, X. Yu, J. Ke, K. Gao, Temperature rise characteristics of the valve-controlled adjustable damping shock absorber, Mechanics & Industry **21**, 111 (2020)